Vol 15 No 12, December 2006
1009-1963/2006/15(12)/3026-07

Chinese Physics

© 2006 Chin. Phys. Soc.
and IOP Publishing Ltd

Critical behaviours and magnetic properties of three-dimensional bond and anisotropy dilution Blume–Capel model in the presence of an applied field*

Yan Shi-Lei(晏世雷)[a)b)†] and Zhu Hai-Xia(朱海霞)[a)c)]

[a)] *Department of Physics, Suzhou University, Suzhou* 215006, *China*
[b)] *Jiangsu Key Laboratory of Thin Films, Suzhou University, Suzhou* 215006, *China*
[c)] *Department of Physics, Yancheng Normal College, Yancheng* 224000, *China*

(Received 9 September 2005; revised manuscript received 17 June 2006)

This paper studies the critical behaviours and magnetic properties of three-dimensional bond and anisotropy dilution Blume–Capel model (BCM) in the presence of an applied field within the effective field theory. The trajectory of tricritical point, reentrant transitions and degenerate patterns of anisotropy are obtained both for the bond and the anisotropy dilutions. The global phase diagrams demonstrate unusually reentrant phenomena. The temperature dependences of magnetization curves undergo remarkable spin glass behaviour at low temperatures, and transform from ferromagnetism to paramagnetism at high temperature in applied fields. Temperature dependence of magnetic susceptibility curve is in qualitative agreement with experimental result.

Keywords: critical behaviours and magnetic properties, Blume–Capel model, bond and anisotropy dilutions, applied field

PACC: 7510D, 7510H, 7510J

1. Introduction

The critical properties of the various spin or pseudo-spin systems have attracted the attention of many workers during the past decades. The Ising model has been one of the most extensively studied models in localized spin systems.[1−4] Though the Ising model is simple but it produces many fruitful results. Since 1966, the Blume–Capel model (BCM) becomes important in the family of Ising models.[5] Its phase diagram presents a line of continuous transition and a line of first-order transition, separated by a tricritical point (TCP). Meanwhile, the BCM is of practical importance, the critical behaviour of ^{3}He-^{4}He mixtures can be described by BCM.[6]. And from the experimental aspects, some studies showed that in the rare-earth fluorides KY_3F_{10} with cubic structure, the magnetic moment displays nearly complete Ising anisotropy along the local symmetry axis. When substituting Dy^{+3}, Er^{+3}, or Yb^{+3} for Y^{+3} in the compound, a transition to the ferromagnetic state occurs with the variation of uniaxial anisotropy.[7,8]

An important development of BCM is the introduction of randomness. The critical behaviour of ^{3}He-^{4}He mixtures in random media has been modelled by BCM with random uniaxial anisotropy.[9] The disordered ferromagnet associated with BCM has been studied by using various techniques, such as mean field theory,[10] renormalization-group method,[11−13] pair approximation,[14] cluster variation method,[15] effective field theory (EFT),[16−18] self-consistent theory,[19] Monte Carlo simulations,[20−22] a sequence of generalized Husimi trees[23] and so on.

It is worthwhile to point out that, for two-dimensional random BCM, the results obtained by means of various techniques are not in complete agreement. Some researches lead to the TCP sudden disappearance,[11,13,14] while others give the TCP gradual depression.[16,17,20] However, for the three-dimensional case, the first-order phase transition is converted to a second-order one above a threshold of random concentration no matter how different techniques are adopted.[12,22] Puha and Diep studied the phase diagrams of three-dimensional bond dilution BCM with random anisotropy by using Monte Carlo simulations and gave some meaningful results.[22]

*Project supported by the Education Bureau Key Natural Science Foundation of Jiangsu Province (Grant No 03KJA140117) and by the Open Foundation of Jiangsu Key Laboratory of Thin Film (Grant No K2022).
†Corresponding author. E-mail: slyan@suda.edu.cn

However, they did not give the global phase diagrams. This is because an obstacle encountered in Monte Carlo simulations on disordered systems is the presence of many metastable states at low temperatures, which is separated by barriers that may diverge in the thermodynamic limit, and make it very hard for the system to equilibrate.

On the other hand, when there exists an applied field, BCM is treated by EFT[24] and mean field theory.[25] In this work, we study critical behaviours and magnetic properties of three-dimensional bond and anisotropy dilution BCM in the presence of an applied field within EFT. Our calculations show rich phase transition messages at low temperatures and distinct magnetic properties, which Monte Carlo simulations do not perform in the same case. The trajectory of the TCP in the phase space is plotted as a function of two different dilution factors. The result is in qualitative agreement with the estimates from the Monte Carlo simulations at high temperatures.[22] The influence of two different dilution factors on critical behaviours is analysed. The temperature dependences of magnetization curves have remarkable spin glass behaviour at low temperatures, and transform from ferromagnetism to paramagnetism at high temperature in applied fields. Temperature dependence of magnetic susceptibility curve is in qualitative agreement with experimental result. To our knowledge, certain above-mentioned subjects are not studied yet.

This paper is organized as follows. In Section 2 we outline the formulae and give some technical points. The detailed numerical results and discussions are given in Section 3. A brief summary is given in Section 4.

2. Formulae

The Hamiltonian for the spin-1 nearest-neighbour interaction bond and anisotropy dilution BCM in the presence of applied field can be defined as

$$H = -\sum_{\langle ij\rangle} J_{ij} S_i^z S_j^z - \sum_i D_i (S_i^z)^2 + H \sum_i S_i^z, \quad (1)$$

where the spins S_i^Z can assume 0 or ± 1 states at each site. The first summation runs only over all pairs of the nearest neighbour sites. The second and third summations involve all sites of lattice. J_{ij} is the exchange interaction between the nearest-neighbour sites and we let $J_{ij} > 0$. D_i represents an anisotropy parameter, which is assumed to be negative. We consider only the case of uniaxial anisotropy (z) axis the same for all the ions. H is a uniform applied field and parallel to the anisotropy (z) axis. J_{ij} and D_i can satisfy independent dilution distributions respectively.

$$P(J_{ij}) = p\delta(J_{ij} - J) + (1-p)\delta(J_{ij}), \quad (2)$$

$$P(D_i) = t\delta(D_i - D) + (1-t)\delta(D_i), \quad (3)$$

where $p_c < p < 1.0$ and $0 < t < 1.0$. Let p denote the bond dilution concentration and t indicate the anisotropy dilution concentration. The p_c is the percolation threshold of bond dilution. We can perform the averaged magnetization m and quadrupolar moment q within the EFT.

$$m = \left[q\langle\cosh(J_{ij}\nabla)\rangle_r + m\langle\sinh(J_{ij}\nabla)\rangle_r + 1 - q\right]^z F(x)|_{x=0}, \quad (4)$$

$$q = \left[q\langle\cosh(J_{ij}\nabla)\rangle_r + m\langle\sinh(J_{ij}\nabla)\rangle_r + 1 - q\right]^z G(x)|_{x=0}, \quad (5)$$

where z is lattice coordination number, $\nabla = \dfrac{\partial}{\partial x}$ is a differential operator. The $\langle\cdots\rangle_r$ denotes the bond dilution average for Eq.(2). The functions $F(x)$ and $G(x)$ are written as:

$$F(x) = \int P(D_i) f(x, D_i) \mathrm{d}D_i, \quad (6)$$

$$G(x) = \int P(D_i) g(x, D_i) \mathrm{d}D_i. \quad (7)$$

The $f(x, D_i)$ and $g(x, D_i)$ are defined as follows:

$$f(x, D_i) = \frac{2\sinh(\beta(x+H))}{2\cosh(\beta(x+H)) + \mathrm{e}^{-\beta D_i}}, \quad (8)$$

$$g(x, D_i) = \frac{2\cosh(\beta(x+H))}{2\cosh(\beta(x+H)) + \mathrm{e}^{-\beta D_i}}, \quad (9)$$

where $\beta = 1/k_B T$. If we combine Eqs.(4),(5), the self-consistent equation with respect to averaged magnetization m is given by

$$m = a_0 + a_1 m + a_2 m^2 + a_3 m^3 + a_4 m^4 + a_5 m^5 + \cdots. \quad (10)$$

The susceptibility can be obtained as

$$\chi_m = \left(\frac{\partial m}{\partial H}\right)_{\rm T}. \tag{11}$$

Although we obtain the self-consistent equation, it is difficult to separate the ferromagnetic state ($m \neq 0$) from the paramagnetic state ($m = 0$) for $H \neq 0$. In this case, we cannot give an expression of phase transition equation. However, when $H = 0$, Eq.(10) is reduced to a simple form,

$$m = a_1 m + a_3 m^3 + a_5 m^5 + \cdots. \tag{12}$$

Since m is small enough near the second-order phase transition line, the expression of second-order phase transition is given by

$$a_1 = 1 \quad \text{and} \quad a_3 < 0. \tag{13}$$

On the critical transition line, there may exist a line of continuous transition and a line of first-order transition, separated by a TCP. When $a_3 > 0$, the phase transition is first-order. Therefore, $a_3 < 0$ must be satisfied. Hence the point at which $a_1 = 1$ and $a_3 = 0$ determines the TCP on the phase transition line. The coefficients a_1 and a_3 are in the following form

$$a_1 = z\langle\sinh(J_{ij}\nabla)\rangle_{\rm r}\left[q_0\langle\cosh(J_{ij}\nabla)\rangle_{\rm r} + 1 - q_0\right]^{z-1} F(x)|_{x=0}, \tag{14}$$

$$\begin{aligned} a_3 = {} & z(z-1)q_1\langle\sinh(J_{ij}\nabla)\rangle_{\rm r}\left[\langle\cosh(J_{ij}\nabla)\rangle_{\rm r} - 1\right]\left[q_0\langle\cosh(J_{ij}\nabla)\rangle_{\rm r} + 1 - q_0\right]^{z-2} F(x)|_{x=0} \\ & + \frac{z(z-1)(z-2)}{3!}\langle\sinh^3(J_{ij}\nabla)\rangle_{\rm r}\left[q_0\langle\cosh(J_{ij}\nabla)\rangle_{\rm r} + 1 - q_0\right]^{z-3} F(x)|_{x=0}, \end{aligned} \tag{15}$$

where q_0 and q_1 satisfy the solutions of

$$q_0 = \left[q_0\langle\cosh(J_{ij}\nabla)\rangle_{\rm r} + 1 - q_0\right]^z G(x)|_{x=0}, \tag{16}$$

$$q_1 = \frac{\frac{z(z-1)}{2!}\left[\langle\sinh(J_{ij}\nabla)\rangle_{\rm r}\right]^2\left[q_0\langle\cosh(J_{ij}\nabla)\rangle_{\rm r} + 1 - q_0\right]^{z-1} G(x)|_{x=0}}{\left\{1 - z\left[\langle\cosh(J_{ij}\nabla)\rangle_{\rm r} - 1\right]\left[q_0\langle\cosh(J_{ij}\nabla)\rangle_{\rm r} + 1 - q_0\right]^{z-1} G(x)|_{x=0}\right\}}. \tag{17}$$

Up to now, we have generalized the expressions for bond and anisotropy dilution BCM in the presence of an applied field. One does not expect to obtain results as precise as those from Monte Carlo simulations. Nevertheless, the EFT procedure can compensate for the defect of Monte Carlo simulations at low temperatures. The order of phase transition is described by the present procedure. Here we consider a simple cubic lattice as the three-dimensional version mainly because the three-dimensional system has experimentally the most relevant dimension.

3. Results and discussions

All the results that will be presented in this section come numerically from solutions of Eqs.(10)–(17).

Firstly, the Curie temperatures versus negative uniaxial anisotropy with concentrations of bond dilution $p = 1.0$, 0.8, and 0.5 for $H = 0$ are depicted in Figs.1(a)–(c) respectively, when the values of anisotropy dilution concentration t are changed. From Fig.1(a), it is clear that, with increasing the anisotropy dilution concentration t, the TCP is depressed monotonically and disappears at a critical concentration t_1^*. The TCP exists only in the ranges of $1.0 > t > t_1^* = 0.784$ and $-3.0 < D/J < -2.81$. The first-order transition disappears only for a finite amount of disorder. This result is in qualitative agreement with the estimates from the Monte Carlo simulations at high temperatures, like Fig.4 in Ref.[22]. For $-2.81 < D/J < 0$, the system is of second-order transition.[18] On the other hand, we see apparently the second-order reentrant transitions in an appropriate range of $t < t_1^*$. Moreover, a special type of reentrant transition line which is called zigzag one can be observed (see curve labelled $t = 0.746$ in Fig.1(a)). The reentrant or zigzag transition comes from the frustration effect and non-uniform convergence of a large uniaxial anisotropy. Certainly, the reentrant phenomena have been found for three-dimensional systems in some other models.[27] Meanwhile, there exist four different values of the uniaxial anisotropy in the range of $t_1^* > t > t_1 = 0.72937$ when Curie temperature

goes to zero. They represent four degenerate patterns of the uniaxial anisotropy at ground state. In this case, all spin states are frozen in a certain range of concentration t. This comes from the fact that the uniaxial anisotropy is parallel to the z axis. The phenomenon does not occur when the uniaxial anisotropy is perpendicular to the z axis.[26] For all $t < t_1$, the second-order transition line extends to $D \to -\infty$ and the critical temperature is finite. This is because the negative infinite anisotropy acting on the given sites tends to force them to be in the states $S = \pm 1$. Thus, the clusters of spin $S = \pm 1$ states are formed and are able to sustain the order for all $t < t_1$. Fig.1(b) shows that the anisotropy dilution concentration scope which affects the TCP becomes large. The TCP exists in the ranges of $1.0 > t > t_2^* = 0.734$ at $p = 0.8$. Obviously, the connectivity of the exchange interactions between all sites is weakened due to the bond dilution. Thus, the uniaxial anisotropy correlation between sites will decline so that we expect the depression of the TCP. Secondly, the bond dilution can strongly depress ordered phase. The role of bond dilution will force some sites from $S = +1$ or $S = -1$ state to $S = 0$ once more. The system must possess a large critical concentration $t_2 = 0.6617$ to form the clusters of $S = \pm 1$ states. By comparing with Figs.1(a), (b), we find some different plots in Fig.1(c). Firstly, there are five values of uniaxial anisotropy in the region $t_3^* = 0.679 > t > t_3 = 0.45873$ when the Curie temperature goes to zero. This is to say that the degenerate patterns appear at ground state. Secondly, we pay attention to the fact that the TCP is depressed greatly. From our calculations, there is TCP in the range $1.0 > p > p_c^* = 0.2954$ for $t = 1.0$. Here, we give its critical value p_c^*. The trajectory of TCP is in qualitative agreement with the result of Monte Carlo simulations at high temperatures, like Fig.7 in Ref.[22].

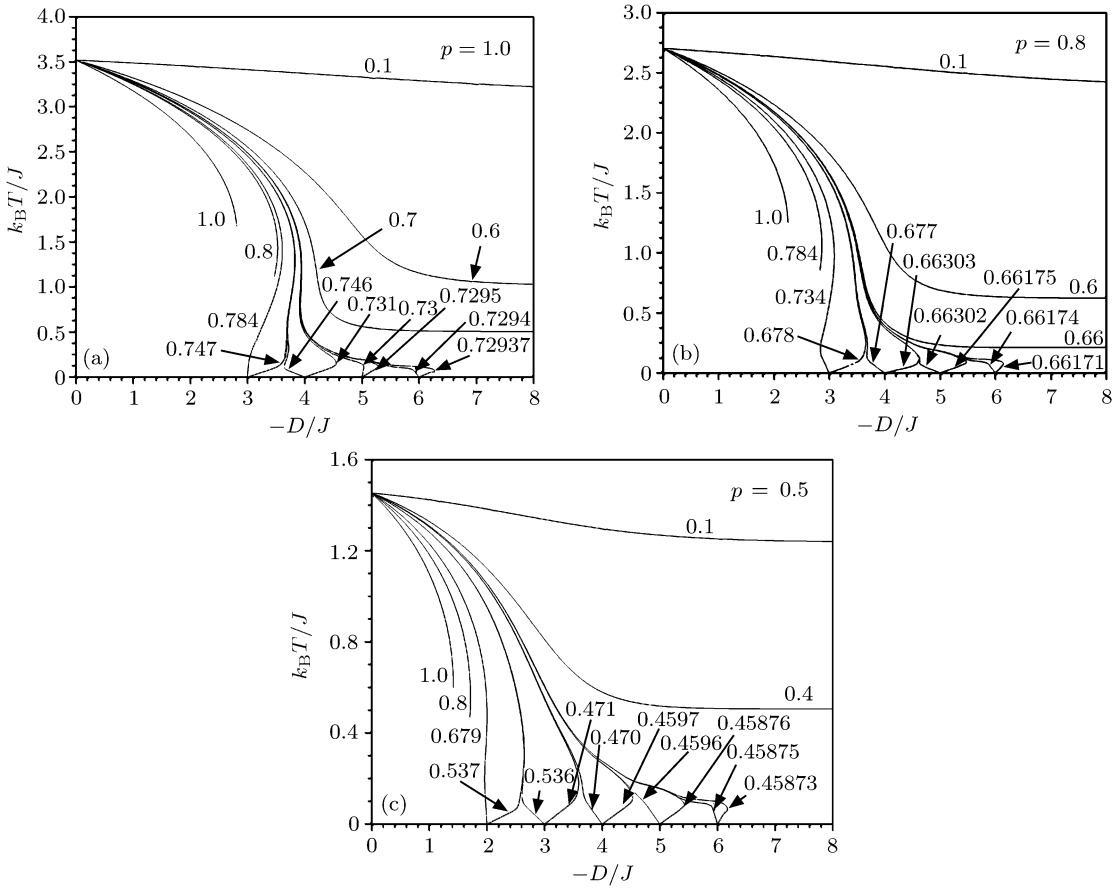


Fig.1. Uniaxial anisotropy dependence of Curie temperature on the simple cubic lattice for different bond concentration $p = 1.0$ (a); 0.8 (b); 0.5(c) is presented. The numbers on the curves are the values of anisotropy dilution concentration t.

Figures 2(a) and (b) illustrate the behaviours of the phase transition as function of bond dilution concentration with $t = 0.8$ and 0.7 for $H = 0$ respectively, when the value of uniaxial anisotropy is changed. Comparing Figs.2(a) and (b), we find that the second-order transition lines exhibit the reentrant phenomena in certain range of a large uniaxial anisotropy, while reentrant phenomena do not occur at all for small ones. However, we find easily that the reentrant phenomena are depressed strongly. Therefore we infer that a large anisotropy dilution concentration can destroy reentrant transition. On the other hand, the ordered phase scopes at low temperatures are enlarged with increasing anisotropy dilution concentration. This comes from degradation of the uniaxial anisotropy effect due to large dilution concentration.

We plot the Curie temperature dependence of the uniaxial anisotropy with a fixed anisotropy dilution concentration $t = 0.75$ in Fig.3, while bond concentration is changed. The phase transition for pure bond status or small bond concentration is the second-order phase transition and the TCP does not exist. When the bond concentration is appropriate, the system shows the TCP. Then the TCP is depressed once more when bond concentration further increases. In this case, the appearance of the TCP is that the bond dilution debases the role of anisotropy between all sites, while a large bond dilution can generate a powerful depression for the TCP again. The trajectories of the TCP dependence of the two different dilution factors have a complex relation. This result displays the overlap correlations between two dilution factors.

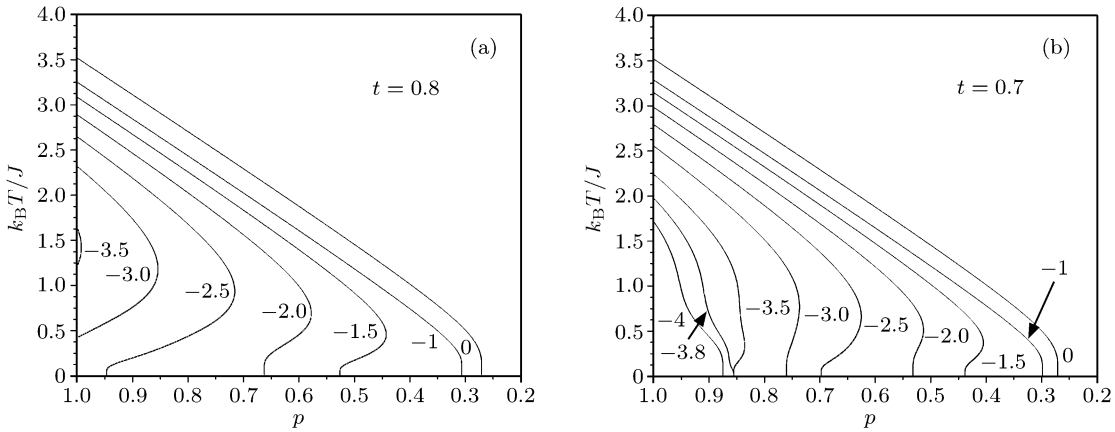


Fig.2. Bond dilution concentration dependence of Curie temperature on the simple cubic lattice for different anisotropy dilution concentration (a) 0.8 and (b) 0.7 is presented. The numbers on the curves are the values of uniaxial anisotropy D/J.

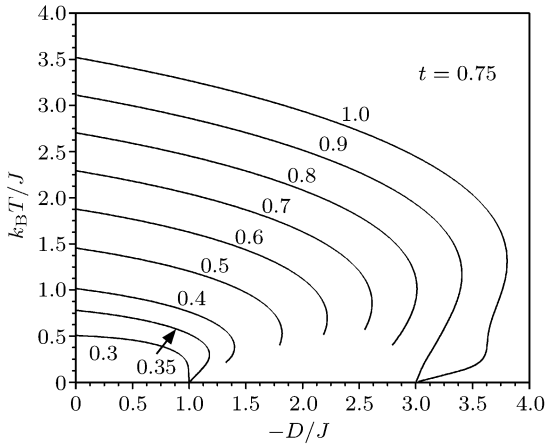


Fig.3. Uniaxial anisotropy dependence of Curie temperature on the simple cubic lattice for a fixed random anisotropy concentration $t = 0.75$ is presented. The numbers on the curves are the values of bond dilution concentration p.

The magnetic property is another important problem. Figure 4 expresses the temperature dependence of the magnetization with $D/J = -3.5$ and $p = 1.0$ for $H = 0$, while the value of anisotropy dilution concentration is changed. Obviously, they express spontaneous magnetizations. The curves increase firstly and then decrease rapidly to zero. Actually, the results reflect the reentrant phenomena corresponding to Fig.1(a) and the existence of spin glass states at low temperatures. When there exists an applied field, the temperature dependence of the magnetizations for $D/J = -4.2$ and $t = 0.73$ at pure bond status is shown in Fig.5. The numbers on the curves are the values of applied field. The magnetization curves have a complex change from $H/J = 0.1$ to 0.4. In fact, they give some important phase transi-

tion messages although the phase diagram is not given in the presence of an applied field. There are the four following conclusions. (1) The degenerate patterns of the uniaxial anisotropy at ground state disappear in applied fields. (2) The complex variation of the magnetization curves represents the existence of reentrant phase transition. In fact, the magnetizations have remarkable spin glass behaviours at low temperatures. (3) A long tail line does not touch the (temperature) axis. This means that the magnetization curves transform from ferromagnetism to paramagnetism at high temperature. (4) When $H/J = 0.5$, the magnetization goes to saturation. The temperature dependence of the magnetization shows monotonous regressive relation due to the existence of a large applied field.

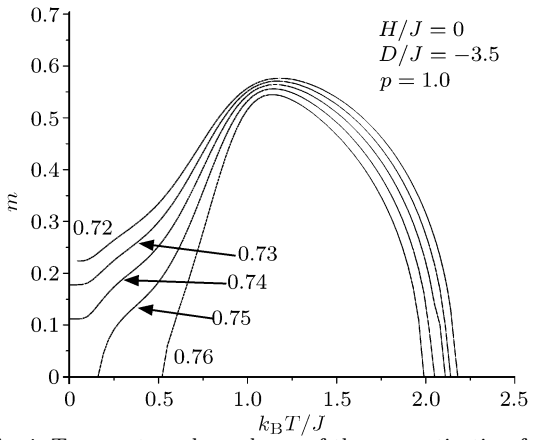


Fig.4. Temperature dependence of the magnetization for a given $D/J = -3.5$ in the absence of an applied field is presented. The numbers on the curves are the values of anisotropy dilution concentration t.

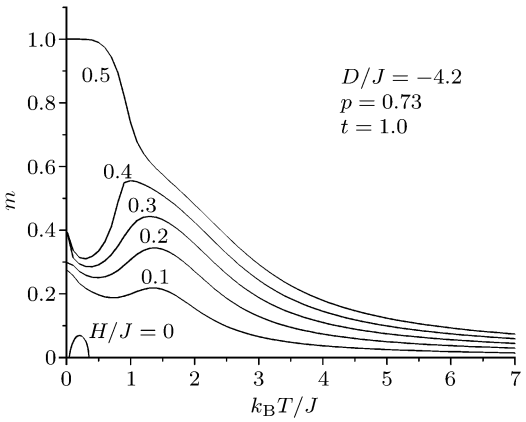


Fig.5. Temperature dependence of the magnetization for a given $D/J = -4.2$ and $t = 0.73$ is presented. The numbers on the curves are the values of applied field H/J.

The initial magnetization curves versus an applied field for a given $k_BT/J = 0.5$, $p = 0.5$ and $t = 1.0$ are depicted in Fig.6.

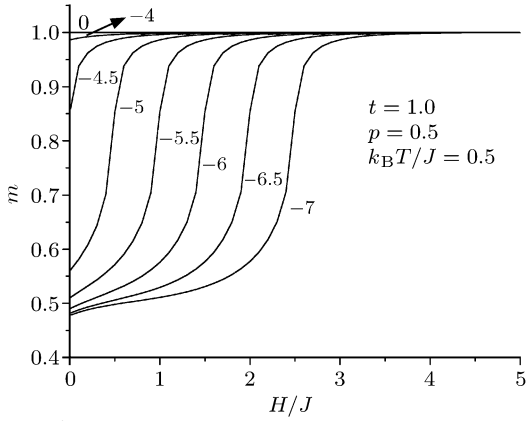


Fig.6. Applied field dependence of the magnetization for a given $k_BT/J = 0.5$, $p = 0.5$ and $t = 1.0$ is presented. The numbers on the curves are the values of uniaxial anisotropy D/J.

The numbers on the curves are the values of uniaxial anisotropy. Here, the initial magnetization curves extend quickly to saturation for small values of anisotropy and go slowly to saturation for large values of anisotropy with increasing applied field. This shows that the existence of uniaxial anisotropy hampers the magnetization process and that the saturation magnetization needs a high-applied field under a large negative uniaxial anisotropy condition. In Fig.7, we study the susceptibility corresponding to above-mentioned initial magnetization curves.

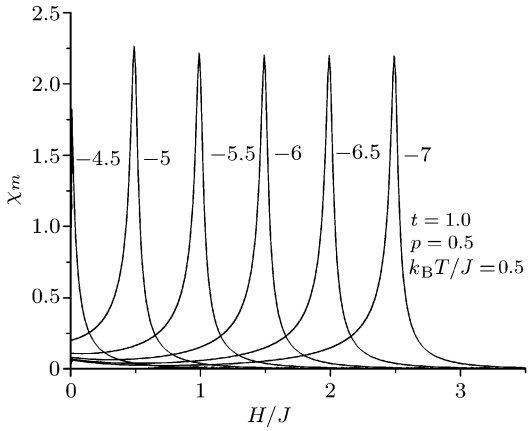


Fig.7. Applied field dependence of the susceptibility for a given $k_BT/J = 0.5$, $p = 0.5$ and $t = 1.0$ is presented. The numbers on the curves are the values of uniaxial anisotropy D/J.

The peak of the susceptibility curve takes place a shift toward large applied field direction with increasing uniaxial anisotropy. There exists only the susceptibility curve in large range of negative uniaxial anisotropy

under the condition of present parameters. This is because initial magnetization goes rapidly to saturation in m-H space for small uniaxial anisotropy. In order to compare with experimental result, the temperature dependence of the inverse susceptibility for a given $D/J = -2.0$, $p = 0.5$ and $t = 1.0$ is presented in Fig.8.

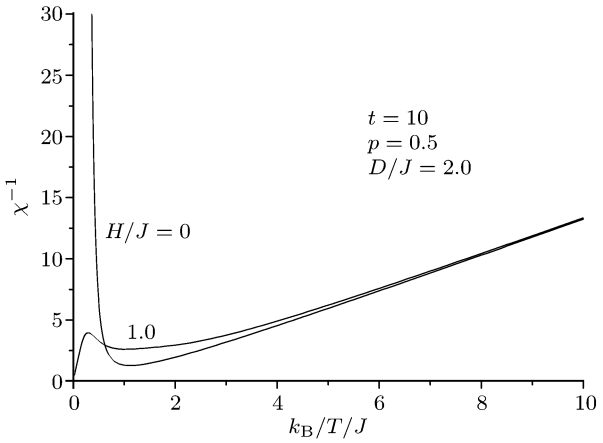


Fig.8. Temperature dependence of the inverse susceptibility for a given $D/J = -2.0$, $p = 0.5$ and $t = 1.0$ is presented. The numbers on the curves are the values of applied field H/J.

We see clearly that theoretical result is in good qualitative agreement with experimental result for $H/J = 1.0$ and is qualitatively consistent with the experimental result for $H/J = 1.0$ at high temperatures, like Fig.5 in Ref.[8]. There is a subtle difference at very low temperatures.

In summary, in this work, we have shown many rich phase transition messages at low temperatures, which are not performed by Monte Carlo simulations.[22] The reentrant phenomenon and the trajectory of the TCP have been discussed. The critical anisotropy and bond dilution concentration is given when the TCP just disappears. The degenerate patterns of uniaxial anisotropy at ground state appear with increasing bond concentration. The temperature dependence of the magnetization has spin glass behaviour at low temperatures and transforms from ferromagnetism to paramagnetism at high temperatures in applied fields. The temperature dependence of the inverse susceptibility curve is in qualitative agreement with experimental result.[8] We hope that the results obtained here may be helpful in further research.

References

[1] Jiang W, Wei G Z, Du A and Zhang Q 2002 *Chin. Phys.* **11** 823

[2] Zhang Y N and Yan S L 2003 *Acta Phys. Sin.* **52** 2890 (in Chinese)

[3] Liang Y Q, Wei G Z, Zhang Q, Qiu W and Zang S L 2004 *Chin. Phys.* **13** 2147

[4] Shao Y Z, Zhong W R, Lin G M and Li J C 2005 *Chin. Phys.* **14** 2110

[5] Blume M 1966 *Phys. Rev.* **141** 517
Capel H W 1966 *Physica* **32** 966

[6] Maritan A, Cieplak M, Swift M R, Toigo F and Banavar J R 1992 *Phys. Rev. Lett.* **69** 221

[7] Chamberlain S L, Luo G and Corruccini L R 2003 *Phys. Rev.* B **67** 134414

[8] Chamberlain S L and Corruccini L R 2005 *Phys. Rev.* B **71** 024434

[9] Buzano C, Maritan A and Pelizzola A 1994 *J. Phys. Condens. Matt.* **6** 327

[10] Carneiro C E I, Henriques V B and Salinas S R 1989 *J. Phys.: Condens. Matt.* **1** 3687

[11] Hui K and Berker A N 1989 *Phys. Rev. Lett.* **62** 2507

[12] Falikov A and Berker A N 1996 *Phys. Rev. Lett.* **76** 4380

[13] Branco N S and Boechat B M 1997 *Phys. Rev.* B **56** 11673

[14] Lara D P and Plascak J A 1998 *Physica* A **260** 443

[15] Ekiz C, Keskin M and Yalcin O 2001 *Physica* A **293** 215

[16] Kaneyoshi T 1992 *Phys. Stat. Sol.* (b) **170** 313

[17] Deng L L and Yan S L 2002 *Chin. Phys.* **11** 481

[18] Zhu H X and Yan S L 2004 *Commun. Theor. Phys.* **44** 789

[19] Grollan S, Kierlik E and Rosinberg M L 2001 *Phys. Rev.* E **63** 131103

[20] Zhang G M and Yang C Z 1993 *Acta Phys. Sin.* **42** 128 (in Chinese)

[21] Deserno M 1997 *Phys. Rev.* E **56** 5204

[22] Puha I and Diep H T 2001 *J. Magn. Magn. Mater.* **224** 85

[23] Monroe J L 2002 *Phys. Rev.* E **65** 026109

[24] Kaneyoshi T, Mielnichi J, Balcerzak T and Wiatrowski G 1990 *Phys. Rev.* B **42** 4388

[25] Borelli M S E and Carneiro C E I 1996 *Physica* A **230** 243

[26] Cherkaoui N, Saber M, El-Atri A and Kerouad M 1999 *Physica* A **272** 144

[27] Branco N S 1996 *Physica* A **232** 477